

Spherical polar coordinate transformation for integration of singular functions on tetrahedra

Michael Carley

November 1, 2021

Abstract

A method is presented for the evaluation of integrals on tetrahedra where the integrand has a singularity at one vertex. The approach uses a transformation to spherical polar coordinates which explicitly eliminates the singularity and facilitates the evaluation of integration limits. The method can also be implemented in an adaptive form which gives convergence to a required tolerance. Results from the method are compared to the output from an exact analytical method and show high accuracy. In particular, when the adaptive algorithm is used, highly accurate results are found for poorly conditioned tetrahedra which normally present difficulties for numerical quadrature techniques.

1 Introduction

The evaluation of singular integrals over volume elements is a numerical operation which arises in a number of fields, in particular where a volume potential is to be computed, such as application of the Biot–Savart law in fluid dynamics and electromagnetism. In these cases, the singularity in the integrand arises from the inverse distance appearing in the Green’s function for the problem, which has a $1/R^\alpha$ dependence.

Given its importance in a number of applications, a number of methods have been developed over the years to evaluate such integrals, including analytical [1, 2, 3, 4, 5, 6, 7], semi-analytical [8], and fully-numerical [9, 10, 11] approaches, among others. In this paper we concentrate on the evaluation of volume integrals on tetrahedra, since these often arise in applications using a structured or unstructured mesh, and because they can be used to evaluate integrals on

other volume elements. The motivation for the work presented is the evaluation of near-field terms in Fast Multipole Method (FMM) accelerated application of the Biot–Savart law on volume meshes, where the far-field interactions can be handled using standard quadratures, but a singular integration scheme is needed to correct for near-field interactions.

Analytical approaches to the problem require an assumption about the variation of source terms on the element. In these cases, the source term is usually modelled as linear, as in methods which use the divergence theorem to reduce the volume integral to a series of line [6] or surface [8] integrals, but monomial source terms of arbitrary order can also be implemented [7]. For many purposes a fully numerical approach is preferable, and a variable transformation is often the most straightforward way to achieve this, as in the method of Khayat and Wilton [10] or the Duffy-type transformations presented by Lv et al. [11].

The approach presented in this paper is purely numerical, requiring no assumptions for interpolation of the source density on the tetrahedron, and uses a transformation to spherical polar coordinates. This is the three dimensional equivalent of the polar transformation used in surface integrals for the Boundary Element Method and has the advantage of explicitly eliminating the singularity without requiring variable transformations as in the well-known Duffy method [9].

The method is based on integration over a tetrahedron in a reference orientation which facilitates the evaluation of the integration limits, Section 2.1. Combined with a transformation relating the reference orientation to the original coordinate system, this gives an algorithm for integration on general tetrahedra. Since this basic algorithm is based on fixed-length quadrature rules it does not give an error estimate. This can be remedied by using the basic algorithm in an adaptive form which can be used to evaluate the volume integral to any required tolerance. Numerical testing and comparison to an exact analytical formulation demonstrate the efficiency and accuracy of the algorithm and in particular of the adaptive algorithm when applied to poorly conditioned tetrahedra.

2 Integration on tetrahedra

We present a method for the evaluation of integrals of the form

$$I = \iiint_V \frac{f(\mathbf{x})}{R^\alpha} dV, \quad (1)$$

on tetrahedra given by nodes \mathbf{x}_i , $i = 0, 1, 2, 3$, with the singularity at node 0 so that

$$R = \|\mathbf{x} - \mathbf{x}_0\| \quad (2)$$

where dV is the element of volume. In the applications which motivate this work, the evaluation of volume potentials, $\alpha = 1, 2$. Other values such as $\alpha = 1/2$ arising in crack mechanics, can be handled by a suitable choice of quadrature rule, and results will also be presented for an irrational value of α close to 3, the limiting case for the integral to be integrable.

2.1 Integration in the reference orientation

Integration is performed on the tetrahedron after transformation to a reference orientation which facilitates the evaluation of integration limits. In this orientation, the tetrahedron is defined by the singular point, taken as the origin, and three nodes \mathbf{y}_i , $i = 1, 2, 3$. A spherical polar coordinate system centred at the origin is used with

$$\mathbf{y} = \rho [\sin \phi \cos \theta, \sin \phi \sin \theta, \cos \phi], \quad (3)$$

noting that $\rho \equiv R$.

In the reference orientation, $\mathbf{y}_1 = [\rho_1, 0, 0]$ and nodes \mathbf{y}_2 and \mathbf{y}_3 are given by

$$\mathbf{y}_2 = \rho_2 [\sin \phi_2 \cos \theta_{23}, \sin \phi_2 \sin \theta_{23}, \cos \phi_2], \quad (4)$$

$$\mathbf{y}_3 = \rho_3 [\sin \phi_3 \cos \theta_{23}, \sin \phi_3 \sin \theta_{23}, \cos \phi_3], \quad (5)$$

that is, the tetrahedron has been transformed so that node 1 lies on the $(\theta, \phi) = (0, \pi/2)$ axis and nodes 2 and 3 lie in the vertical plane given by $\theta = \theta_{23}$. The integral over the tetrahedron is then

$$I = \iiint \frac{f(\mathbf{x})}{R^\alpha} d\mathbf{y} = \int_0^{\theta_{23}} \int_{\phi_2(\theta)}^{\phi_3(\theta)} \int_0^{\rho(\theta, \phi)} f(\mathbf{x}) \rho^{n+\gamma} d\rho \sin \phi d\phi d\theta, \quad (6)$$

$$n + \gamma = 2 - \alpha,$$

where $\phi_2(\theta)$ is the value of ϕ at which the vertical plane with azimuthal angle θ intersects the line joining nodes 1 and 2, and likewise for $\phi_3(\theta)$. In order to handle non-integer values of α , we introduce the notation $n + \gamma = 2 - \alpha$, where n is an integer and $-1 \leq \gamma \leq 1$, where γ will be used later to define the weighting function of a Gauss-Jacobi quadrature.

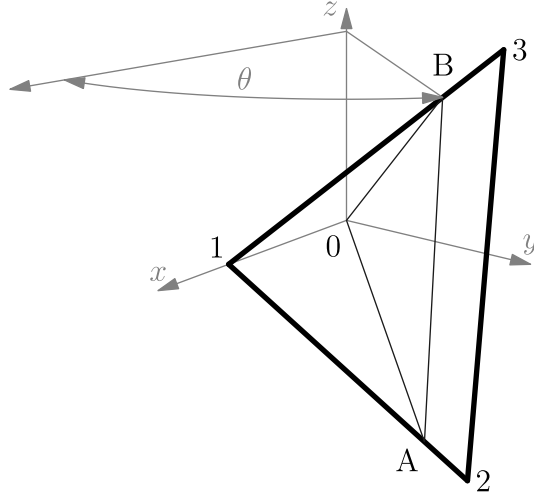


Figure 1: Calculation of integration limits as intersections of plane through origin with face 123 of tetrahedron

The calculation of the limits in ϕ and ρ requires two simple calculations for the intersection of a plane with a line, and of two lines. Figure 1 shows the geometry of the system. At azimuthal angle θ , the integration limits in ϕ are determined by the intersection of the plane of constant θ with the edges 12 and 13, denoted A and B respectively. The intersection point is given by

$$\mathbf{y}_A = \mathbf{y}_1 + (\mathbf{y}_2 - \mathbf{y}_1)u, \quad (7)$$

$$u = -\frac{\mathbf{y}_1 \cdot \mathbf{s}}{(\mathbf{y}_2 - \mathbf{y}_1) \cdot \mathbf{s}}, \quad (8)$$

$$\mathbf{s} = [\sin \theta, -\cos \theta, 0],$$

with a similar calculation to find \mathbf{y}_B . Integration over ϕ is then performed for $\phi_A \leq \phi \leq \phi_B$ with ϕ_A and ϕ_B ordered so that $\phi_A < \phi_B$.

For a given direction (θ, ϕ) , the limit on ρ is determined by the intersection of the ray through the origin with the line segment AB. The distance from the origin to this intersection is given by

$$\rho = \frac{\rho_A \rho_B \sin(\phi_A - \phi_B)}{(\rho_B \cos \phi_B - \rho_A \cos \phi_A) \sin \phi - (\rho_B \sin \phi_B - \rho_A \sin \phi_A) \cos \phi}. \quad (9)$$

Integration on the tetrahedron can then be performed by integrating over θ , evaluating the limits of the inner integrals at each point.

2.2 Transformation to reference orientation

In the previous section a simple method of evaluating the singular integral on a tetrahedron in a reference orientation was presented. Given a point \mathbf{y} on the tetrahedron, the integrand $f(\mathbf{x})/\rho^\alpha$ can be evaluated using the rotation matrix connecting the original and reference coordinate systems and a translation of the origin,

$$\mathbf{x} = \mathbf{x}_0 + \mathbf{y}\mathbf{A}, \quad (10)$$

where \mathbf{A} is the rotation matrix.

The approach taken to transforming between coordinate systems is to construct the transformed tetrahedron and then solve for \mathbf{A} . Given the original tetrahedron nodes \mathbf{x}_i , $i = 0, 1, 2, 3$, we define $\ell_1 = \|\mathbf{x}_1 - \mathbf{x}_0\|$ and set the first node of the transformed tetrahedron $\mathbf{y}_1 = [\ell_1, 0, 0]$. Nodes 2 and 3 are positioned using the constraint that the angle between line 01 and the plane containing the triangle 023 must be the same in both coordinate systems. This is achieved by the following procedure. First, calculate the normal to the plane containing triangle 023, the projection \mathbf{p} of node 1 onto that plane, and construct a coordinate system centred at \mathbf{p} . Writing $\mathbf{x}'_i = \mathbf{x}_i - \mathbf{x}_0$,

$$\hat{\mathbf{n}} = \frac{\mathbf{x}'_3 \times \mathbf{x}'_2}{\|\mathbf{x}'_3 \times \mathbf{x}'_2\|}, \quad (11)$$

$$d = \mathbf{x}'_1 \cdot \hat{\mathbf{n}}, \quad (12)$$

$$\mathbf{p} = \mathbf{x}'_1 - d\hat{\mathbf{n}}, \quad (13)$$

$$\hat{\mathbf{s}} = \mathbf{p}/\|\mathbf{p}\|, \quad (14)$$

$$\hat{\mathbf{t}} = \hat{\mathbf{n}} \times \hat{\mathbf{s}}. \quad (15)$$

This yields a coordinate system centred at point \mathbf{p} with unit vectors $\hat{\mathbf{s}}$, $\hat{\mathbf{t}}$, and $\hat{\mathbf{n}}$, with the first two axes lying in the plane, and the third being the normal to it. The angle between the edge 01 and the plane 023 is then given by

$$\theta_{23} = \cos^{-1} \frac{\mathbf{x}_1 \cdot \hat{\mathbf{s}}}{\ell_1}. \quad (16)$$

To construct nodes 2 and 3 in the rotated coordinate system, we establish a corresponding set of axes for the 023 plane as follows,

$$\hat{\mathbf{n}}' = [-\sin \theta_{23}, \cos \theta_{23}, 0], \quad (17)$$

$$d' = \mathbf{y}_1 \cdot \hat{\mathbf{n}}' = -\ell_1 \sin \theta_{23}, \quad (18)$$

$$\mathbf{p}' = \mathbf{y}_1 - d'\hat{\mathbf{n}}', \quad (19)$$

$$\hat{\mathbf{s}}' = \mathbf{p}'/\|\mathbf{p}'\|, \quad (20)$$

$$\hat{\mathbf{t}}' = \hat{\mathbf{n}}' \times \hat{\mathbf{s}}'. \quad (21)$$

This gives a coordinate system based on a plane with the correct orientation with respect to \mathbf{y}_1 and allows the calculation of nodes 2 and 3 as,

$$\mathbf{y}_i = \mathbf{p}' + \hat{\mathbf{s}} \cdot (\mathbf{x}'_i - \mathbf{p}) \hat{\mathbf{s}}' + \hat{\mathbf{t}} \cdot (\mathbf{x}'_i - \mathbf{p}) \hat{\mathbf{t}}'. \quad (22)$$

The rotation matrix \mathbf{A} is then found by solving

$$\begin{bmatrix} \mathbf{y}_1 \\ \mathbf{y}_2 \\ \mathbf{y}_3 \end{bmatrix} \mathbf{A} = \begin{bmatrix} \mathbf{x}'_1 \\ \mathbf{x}'_2 \\ \mathbf{x}'_3 \end{bmatrix}, \quad (23)$$

for \mathbf{A} .

Algorithm 1 gives pseudocode for the evaluation of the integral on a tetrahedron defined by four nodes \mathbf{x}_i , $i = 0, \dots, 3$, with the singularity at node 0. Required inputs are Gauss-Legendre quadrature rules $(t_i^{(\theta)}, w_i^{(\theta)})$, $(t_j^{(\phi)}, w_j^{(\phi)})$, for integration over θ and ϕ , respectively. Integration over ρ is accomplished using a Gauss-Jacobi rule $(t_k^{(\rho)}, w_k^{(\rho)})$ with weight function $(1+t)^\gamma(1-t)^0$. For integer values of α , $\gamma \equiv 0$ and a Gauss-Legendre rule can be used. Rules are given as N_θ nodes $t_i^{(\theta)}$ and weights $w_i^{(\theta)}$, etc, with $-1 < t_i^{(\theta)} < 1$.

Algorithm 1 Pseudocode for integration on tetrahedron

```

generate tetrahedron in reference orientation  $\mathbf{y}_i$  and solve for rotation matrix  $\mathbf{A}$ 
set  $I = 0$ 
set  $\bar{\theta} = \theta_{23}/2$ ,  $\Delta\theta = \theta_{23}/2$ 
for  $i = 1, \dots, N_\theta$  do calculate  $\theta_i = \bar{\theta} + \Delta\theta t_i^{(\theta)}$ 
  calculate  $\phi_A(\theta_i)$ ,  $\phi_B(\theta_i)$  from Equation 7
  set  $\bar{\phi} = (\phi_A + \phi_B)/2$ ,  $\Delta\phi = \|\phi_A - \phi_B\|/2$ 
  for  $j = 1, \dots, N_\phi$  do calculate  $\phi_j = \bar{\phi} + \Delta\phi t_j^{(\phi)}$ 
    calculate  $\rho_{ij}(\theta_i, \phi_j)$  from Equation 9
    for  $k = 1, \dots, N_\rho$  do calculate  $\rho_{ijk} = \rho_{ij}(1 + t_k^{(\rho)})/2$ 
      set  $\mathbf{y}_{ijk} = \rho_{ijk}[\cos \theta_i \sin \phi_j, \sin \theta_i \sin \phi_j, \cos \phi_j]$ 
      set  $\mathbf{x} = \mathbf{x}_0 + \mathbf{y}\mathbf{A}$ 
      set  $I := I + f(\mathbf{x}) \rho_{ijk}^n \sin \phi_j \Delta\theta \Delta\phi \left(\frac{\rho_{ij}}{2}\right)^{\gamma+1} w_i^{(\theta)} w_j^{(\phi)} w_k^{(\rho)}$ 
    end for
  end for
end for

```

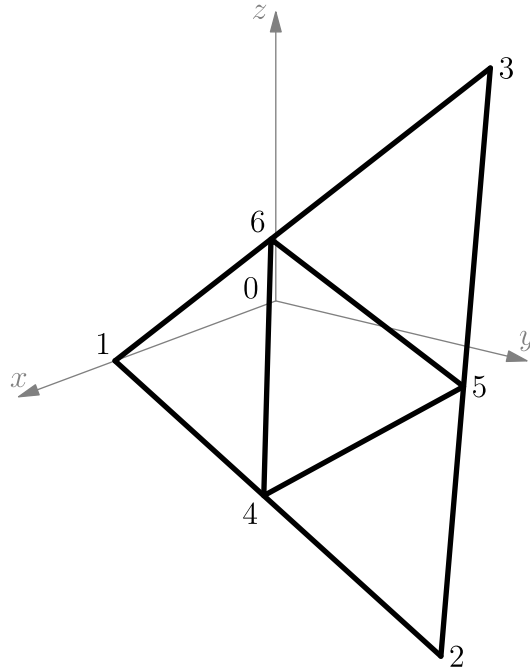


Figure 2: Splitting a tetrahedron for adaptive quadrature

2.3 Adaptive quadrature

The basic algorithm of the previous section is easily implemented and reliable for “well-shaped” tetrahedra. It does, however, have the drawback that it gives no indication of the accuracy of the result meaning that the user must either accept the possibility of uncontrolled errors in the calculated value of the integral, or use excessively high order quadrature rules with correspondingly excessive computational effort. In this section, we give a method for using the algorithm as the basis of an adaptive technique which can be used to give results correct to some stated tolerance and which allow the approach to be used with confidence on tetrahedra which are poorly conditioned.

The procedure consists of splitting the face 123 into four new triangles by bisecting each edge, as shown in Figure 2, and integrating over the resulting sub-tetrahedra using the algorithm of the previous section. Given a tolerance ϵ , the convergence test is to check

$$\left\| I_0 - \sum_{i=1}^4 I_i \right\| \leq \epsilon, \quad (24)$$

where I_0 is the integral evaluated on the original tetrahedron, and I_i , $i = 1, 2, 3, 4$ is the integral on each sub-tetrahedron. Sub-tetrahedra

are 0146, 0425, 0536, and 0456. If the convergence criterion is not met, the sub-tetrahedra are split and the algorithm is applied recursively until the estimate of the total converges to the required tolerance. In the next section, the effectiveness of this adaptive procedure will be demonstrated.

3 Results

Results are presented to demonstrate the performance of the quadrature algorithm in computing integrals over tetrahedra of various shapes. The first test integrals, which correspond to the evaluation of a volume potential such as the Biot–Savart law, are

$$I_{ijk} = \iiint \frac{x^i y^j z^k}{R^\alpha} dx dy dz, \quad i + j + k \leq N, \quad (25)$$

computed for $0 \leq N \leq 4$, with $\alpha = 1$. The relative error is given as

$$\epsilon_{\text{rel}} = \max_{ijk} \frac{\|I_{ijk} - J_{ijk}\|}{\|J_{000}\|}, \quad (26)$$

where J_{ijk} is the exact value found using an analytical method [7].

The test geometries are chosen for comparison with previous work on a Duffy transformation method [11] and test the algorithms on tetrahedra whose geometries cause difficulties for numerical evaluation.

3.1 Basic algorithm

We first present results to assess the performance of the basic algorithm. The length of the Gauss-Legendre rules is varied, with $N_\theta = N_\phi = N_\rho$ in each calculation. For compatibility with previous work [11], three tetrahedra are considered. The first has nodes $\mathbf{x}_0 = [0, 0, h]$, $\mathbf{x}_1 = [0, 0, 0]$, $\mathbf{x}_2 = [0, 1, 0]$, and $\mathbf{x}_3 = [1, 1, 0]$, with the height h varied to examine the effect on the quadrature error. The second and third cases consider variations in the geometry of the base of the tetrahedron, Figure 3, to study possible effects of poorly-conditioned elements. In these cases, the node $\mathbf{x}_0 = [0, 0, 0.1]$. In the second case, $\mathbf{x}_3 = [\sin \theta, 1 - \cos \theta, 0]$ to study the influence of the vertex angle on the tetrahedron base. In the final test, the effect of the base aspect ratio is considered, by setting $\mathbf{x}_3 = [a, 1, 0]$ and varying a .

Figure 4 shows the effect of varying the tetrahedron geometry on the computational effort required to achieve a given accuracy. As might be expected, in the case of a “well-conditioned” tetrahedron,

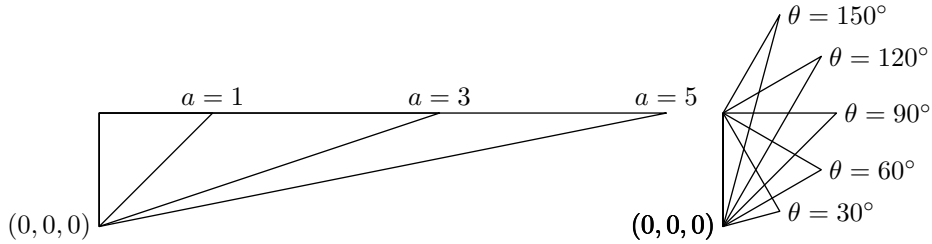


Figure 3: Variation of tetrahedron base geometry: left hand side, aspect ratio variation; right hand side, vertex angle variation

$h \approx 1$ in the upper plot, convergence is rapid and machine precision can be achieved. As h is reduced, however, the method cannot achieve high accuracy with the number of quadrature points available and has quite poor results for $h = 0.05$. In the other two plots, the value of h is held constant at 0.1 and the shape of the tetrahedron base is varied. Again, as the tetrahedron becomes more poorly conditioned, because of changes to the vertex angle or to the base aspect ratio, the quadrature scheme shows poor accuracy and unreliable convergence. The results of the next section will show how the adaptive version of the algorithm can overcome these defects and allow the method to converge to a required tolerance.

3.2 Adaptive algorithm

Results for the adaptive version of the algorithm are presented in Figure 5. In this case the tetrahedron nodes are $\mathbf{x}_0 = [0, 0, h]$, $\mathbf{x}_1 = [0, 0, 0]$, $\mathbf{x}_2 = [0, 1, 0]$, and $\mathbf{x}_3 = [2, 1, 0]$ with h being changed to modify the conditioning of the tetrahedron. As before, an exact method is used to evaluate the integrals on the resulting tetrahedra. The adaptive algorithm is applied for three tolerances, $\epsilon = 10^{-3}, 10^{-6}, 10^{-9}$ and using Gaussian quadrature rules of length $N_\theta = 4, 8, \dots, 20$. Results presented are the total number of function evaluations required at each recursion level to reach the requested tolerance as a function of the tetrahedron conditioning represented by the height h .

The results show the expected convergence behaviour. For $h \approx 1$, any of the quadrature rules gives a solution to the required tolerance, as for the basic algorithm evaluated in the previous section, but as h is reduced and the tetrahedron becomes more poorly conditioned, the method needs a greater number of recursions to achieve convergence. At small values of h and $\epsilon = 10^{-9}$, this leads to a large number of function evaluations. In all cases, however, the requested tolerance is achieved, even when quite low-order Gaussian quadratures, $N = 4, 8$,

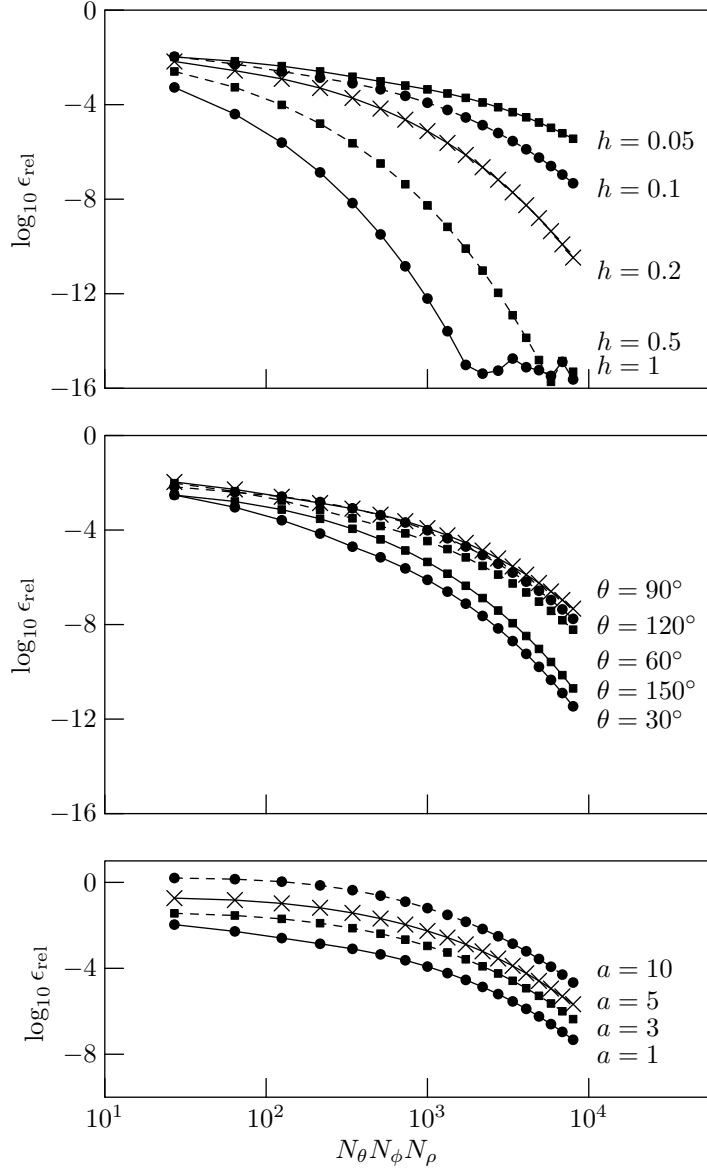


Figure 4: Effect of varying tetrahedron geometry on integration accuracy, error against total number of function evaluations; from top: varying tetrahedron height h , vertex angle θ , base aspect ratio a .

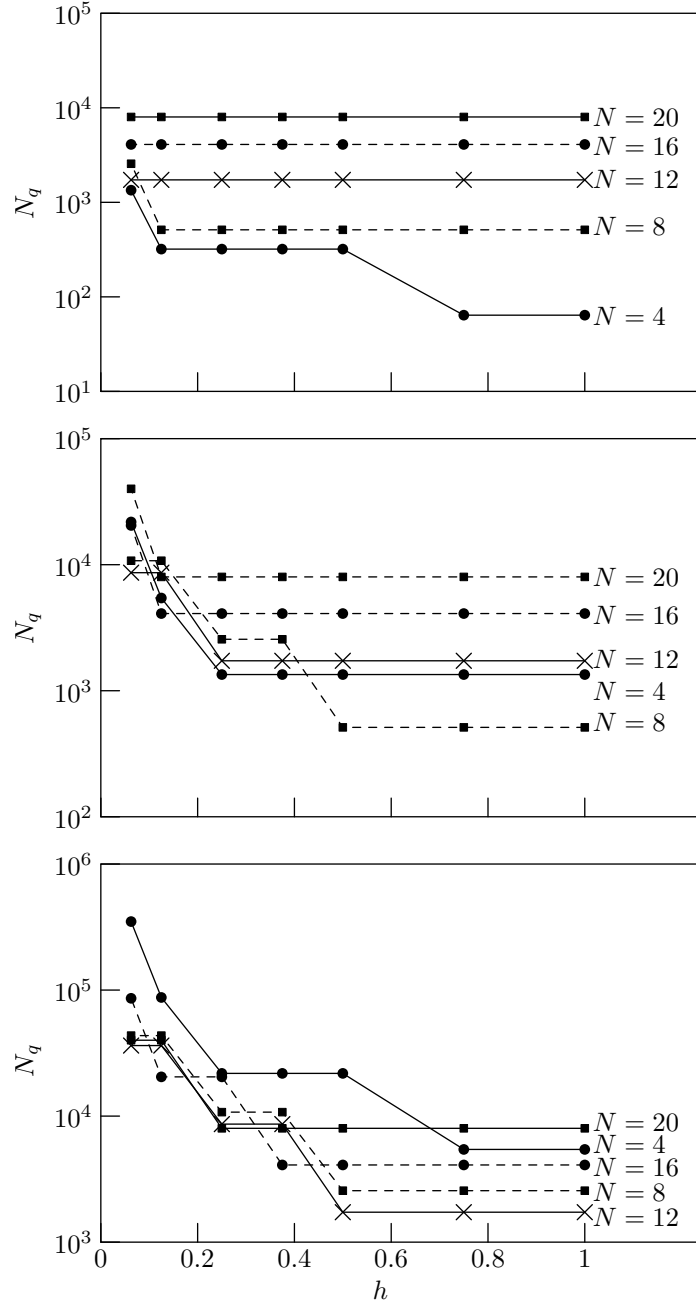


Figure 5: Effect of varying tetrahedron height on number of quadrature points at fixed tolerance using adaptive quadrature, total number of function evaluations against height h ; from top: tolerance $\epsilon = 10^{-3}, 10^{-6}, 10^{-9}$.

are used to integrate on sub-elements. Numerical tests for accuracy when the base shape is modified give similar results with convergence roughly independent of aspect ratio a and vertex angle θ and are not presented here.

It is interesting to note that the low-order rules can require more function evaluations to achieve a given tolerance than higher order rules, in particular, for $h \approx 1$. This appears to happen because for the well-conditioned tetrahedron, the low-order rules can require more recursion levels to reach the convergence criterion.

We hypothesize that the adaptive algorithm achieves good convergence because the base splitting shown in Figure 2 has the effect of generating four tetrahedra which are better conditioned than the parent element by virtue of having smaller area bases with a constant height, in effect increasing h with a corresponding improvement in the element conditioning.

3.3 Non-integer α

The previous sections show how the proposed algorithm works for an integrand with integer α , where a reference value can be evaluated exactly using analytical methods. This is an important case in many applications, but there are also problems where non-integer values appear. Here, we consider two cases, $\alpha = 1/2$ which arises in crack problems in solid mechanics, and an irrational value of α which poses particular difficulties for coordinate transformation schemes.

In the first case, that of rational α , a Duffy-type transformation [11] can eliminate the singularity and allow Gauss-Legendre rules to be used in the radial direction. Figure 6 shows the performance of the method compared to the evaluation of a reference integral using a Duffy-type method which has been found reliable for this case [11]. The integral is evaluated on a tetrahedron with nodes $\mathbf{x}_0 = [0, 0, 1/2]$, $\mathbf{x}_1 = [0, 0, 0]$, $\mathbf{x}_2 = [0, 1, 0]$, and $\mathbf{x}_3 = [1, 1, 0]$. The Duffy transformation was applied to the integral using high-order Gauss-Legendre rules to give a reference value, and the method of this paper was implemented using Gauss-Legendre rules in θ and ϕ and a Gauss-Jacobi rule for ρ .

Finally, we consider a case similar to that used in previous work [12], with an irrational value of α which is close to the point where the integrand is not integrable. We set $\alpha = 3 - 1/\pi$ and integrate using a quadrature with $\gamma = 1/\pi - 1 \approx -0.6817$. This integral cannot be evaluated using the Duffy-type coordinate transformation so convergence is tested by evaluating

$$\delta = \|I - I_{(\text{ref})}\|, \quad (27)$$

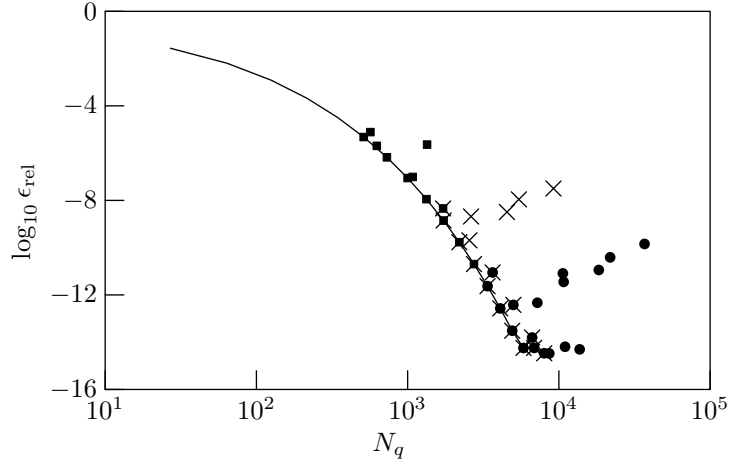


Figure 6: Convergence of algorithm for $\alpha = 1/2$: error versus number of function evaluations. Solid line: basic algorithm; squares, adaptive algorithm with $\epsilon = 10^{-6}$; crosses, adaptive algorithm with $\epsilon = 10^{-9}$; bullets, adaptive algorithm with $\epsilon = 10^{-12}$

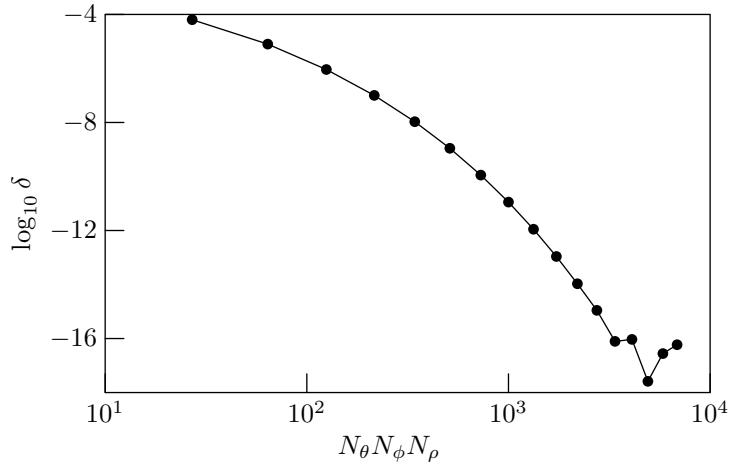


Figure 7: Convergence of algorithm for $\alpha = 3 - 1/\pi$: difference between integral and reference versus number of function evaluations for basic algorithm.

where I_{ref} is the integral evaluated using quadrature rules of length 20, or $20^3 = 8000$ function evaluations, in the Duffy-type approach. Figure 7 shows δ against the total number of function evaluations for the same tetrahedron geometry as in Figure 6. In order to track the convergence of the integral, a single monomial source term is used, evaluating I_{111} as defined in Equation 25.

The convergence shown by Figure 7 is quite rapid, even for this demanding case, and is comparable to the convergence shown in the corresponding plot in Figure 4. The Gauss-Jacobi rule handles the singularity in the integrand and convergence to machine precision is achieved.

4 Conclusions

A method has been presented for the evaluation of integrals on a tetrahedron with a singularity at one vertex, motivated by the evaluation of volume integrals used in fluid dynamics and electromagnetism, and in fracture mechanics. The algorithm has been shown to be reliable for well-conditioned tetrahedra in its basic form. Extended to an adaptive form, it can compute the volume integral to a required tolerance, even when the tetrahedron is poorly conditioned. The method uses standard tools, such as one-dimensional Gauss quadratures and simple geometric transformations, and can be used without difficulty in production codes.

References

- [1] Urankar, L.K.: Vector potential and magnetic field of current-carrying finite arc segment in analytical form, part IV: General three-dimensional current density. *IEEE Transactions on Magnetics* **20**(6), 2145–2150 (1984)
- [2] Weggel, C.F., Schwartz, D.P.: New analytical formulas for calculating magnetic field. *IEEE Transactions on Magnetics* **24**(2), 1544–1547 (1988)
- [3] Onuki, T., Wakao, S.: Systematic evaluation for magnetic field and potential due to massive current coil. *IEEE Transactions on Magnetics* **31**(3), 1476–1479 (1995)
- [4] Graglia, R.D.: Static and dynamic potentials for linearly varying source distributions in two- and three-dimensional problems. *IEEE Transactions on Antennas and Propagation* **AP-35**(6), 662–669 (1987)

- [5] Wilton, D.R., Rao, S.M., Glisson, A.W., Schaubert, D.H., Al-Bundak, O.M., Butler, C.M.: Potential integrals for uniform and linear source distributions on polygonal and polyhedral domains. *IEEE Transactions on Antennas and Propagation* **AP-32**(3), 276–281 (1984)
- [6] Suh, J.-C.: The evaluation of the Biot–Savart integral. *Journal of Engineering Mathematics* **37**, 375–395 (2000). <https://doi.org/10.1023/A:1004666000020>
- [7] Carley, M., Angioni, S.: Exact integration of surface and volume potentials. *Journal of Engineering Mathematics* **104**, 93–106 (2017). <https://doi.org/10.1007/s10665-016-9875-5>
- [8] Marshall, J.S., Grant, J.R., Gossler, A.A., Huyer, S.A.: Vorticity transport on a Lagrangian tetrahedral mesh. *Journal of Computational Physics* **161**(1), 85–113 (2000). <https://doi.org/10.1006/jcph.2000.6490>
- [9] Duffy, M.G.: Quadrature over a pyramid or cube of integrands with a singularity at a vertex. *SIAM Journal of Numerical Analysis* **19**(6), 1260–1262 (1982)
- [10] Khayat, M.A., Wilton, D.R.: Numerical evaluation of singular and near-singular potential integrals. *IEEE Transactions on Antennas and Propagation* **53**(10), 3180–3190 (2005). <https://doi.org/10.1109/TAP.2005.856342>
- [11] Lv, J.-H., Jiao, Y.-Y., Feng, X.-T., Wriggers, P., Zhuang, X.-Y., Rabczuk, T.: A series of Duffy-distance transformation for integrating 2D and 3D vertex singularities. *International Journal for Numerical Methods in Engineering* **118**, 38–60 (2019). <https://doi.org/10.1002/nme.6016>
- [12] Chernov, A., von Petersdorff, T., Schwab, C.: Quadrature algorithms for high dimensional singular integrands on simplices. *SIAM Journal of Numerical Analysis* **70**, 847–874 (2015). <https://doi.org/10.1007/s11075-015-9977-6>